Published in "Advanced Optical Materials doi: 10.1002/adom.201300415, 2013"
which should be cited to refer to this work.

http://doc.rero.ch

Supporting Information for

Silicon Hyperuniform Photonic Materials with a Pronounced Gap in the Shortwave Infrared.

*Nicolas Muller, Jakub Haberko, Catherine Marichy and Frank Scheffold**

Nicolas Muller, Dr. Jakub Haberko, Dr. Catherine Marichy, Prof. Frank Scheffold
Department of Physics and Fribourg Center for Nanomaterials, University of Fribourg, Chémin du Musée 3, 1700 Fribourg, Switzerland; E-mail: (Frank.Scheffold@unifr.ch)
Dr. Jakub Haberko, Faculty of Physics and Applied Computer Science, AGH University of Science and Technology, al. Mickiewicza 30, 30-059 Krakow, Poland

1. Thermogravimetric analysis of the polymer photoresist.

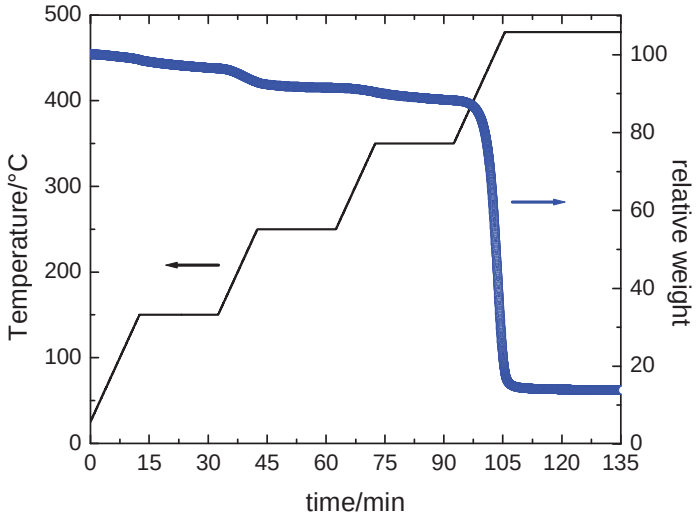

Figure SI-1 Thermogravimetric analysis of the UV-cured IP-Dip photoresist under inter (N_2) atmosphere. Solid line: Temperature. Symbols: relative weight in per cent.

2. Electron micrograph of pure TiO_2 network structure

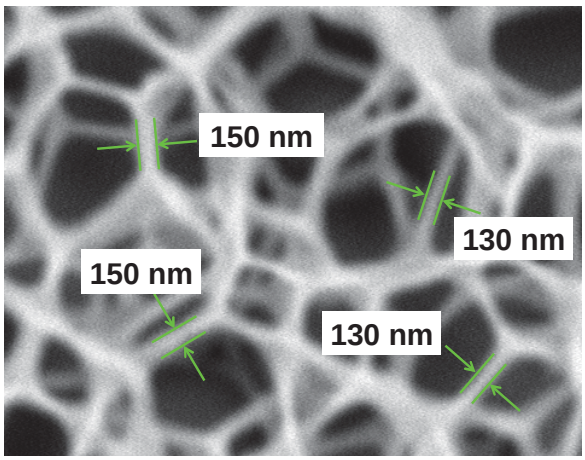

Figure SI-2. Scanning electron microscopy of a TiO_2 network structure h=6μm obtained after high temperature vacuum annealing of the TiO_2 coated polymer structure without addition of the Disilane precursor (for details see experimental section). The short axis oft he cylindrical rods (in plane) is approximately 130-150nm and therefore $\langle D \rangle \sim 220 - 250$nm for an aspect ratio of 2.8.

3. Electron micrograph of the entire sample before and after infiltration

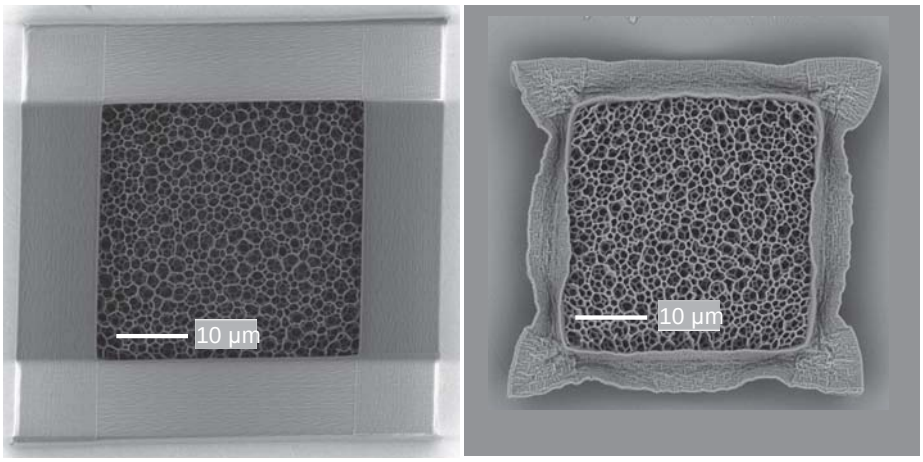

Figure SI-3. Left: Scanning electron microscopy of a typical polymer template h=6µm stabilized by a massive rectangular wall. Right: Same type of structure after the final silicon infiltration step (infiltration time 9 min). The images reveal the high quality of the material. The polymer template, including the massive wall, has been (almost) entirely degraded during the thermal treatment prior to the 480°C silicon CVD while the hyperuniform network structure in silicon is perfectly retained. Electron micrographs are shown at the same magnification and the scale bar is 10µm in both cases.

4. Elemental analysis of Si-TiO_2 HU structure.

Energy Dispersive Spectroscopy (EDS) on Silicon coated TiO_2 hyperuniform (HU) structures confirms the presence of TiO_2 and Si. The spectrum (Figure S3) recorded from a FIB cross-section highlights the presence of Si atoms as well as Ti and O atoms. Calcium and fluoride atoms arise from the glass substrate and a contamination with gallium is noticed during the FIB cross-section process. The quantitative values shown in Table S1 permit to verify the formation of TiO_2 and Si during the different steps. Indeed, the atomic percentage of O being approximately twice that Ti is coherent with the presence of TiO_2. The excess of O atoms can be attributed to adsorption or slight Si surface oxidation when the structure is exposed to air, which should not exceed 1-2 %. In order to avoid charging effects, graphite bridges were formed close to the structure to the sample holder. The observed carbon can thus be attributed to the graphite deposited for the SEM observation and to contamination in air but could also be partially due to residual carbonized polymer.

From the weight fraction of Ti and O (18.37%) and Si (44.7%) we can estimate the volume fraction of the TiO_2 core in the Si coated rods. The mass density of amorphous silicon is 2.32 g/cm^3 and the reference value for bulk TiO_2 is 4.26g/cm^3, however in the literature values for amorphous and crystalline TiO_2 can be found between 2.9 and 3.9 g/cm^3. We thus estimate

http://doc.rero.ch

the volume fraction of the TiO_2 in the rods, after 9 min of Si infiltration, to be in the range of 22-33%. The latter is consistent with a TiO_2 volume fraction of $\phi_0 \sim 4\%$ and a total volume filling fraction of $\phi \sim 15\%$.

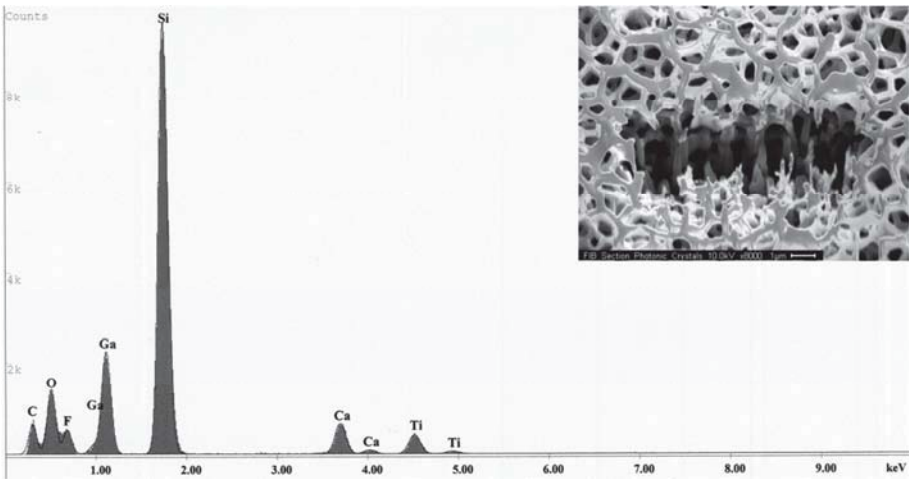

Figure SI-4. EDS spectra of Si-TiO_2 HU structure, recorded from the cross-section shown in the SEM image in inset.

Table SI-1. Elemental analysis of Si-TiO_2 HU structure, by EDS, on a FIB cross-section shown in Figure S3.

Element	Atomic (%)	Weight (%)
Carbon (K)	22.95	10.20
Oxygen (K)	13.49	7.98
Titanium (K)	5.87	10.39
Silicon (K)	43.03	44.70
Fluoride (K)	2.32	1.63
Calcium (K)	6.15	9.11
Gallium (L)	6.20	15.98
Total	100.00	100.00

The energy-level shell used for the analysis is indicated in brackets close to each element.

5. Infrared spectroscopy study of the sample at different fabrication stages

In Figure S4, taken from the polymer template, typical vibration bands of the polymer functional groups are visible (dark grey line). After TiO_2 ALD, the same characteristic signature of the polymer is observed, (light grey line), while after Si CVD (black line) all these bands are disappeared. Indeed, at the Si deposition temperature, the polymer decomposes and one can conclude that the polymer is (almost entirely) removed in the gas stream as a by-product. This is scenario is also supported by the almost complete removal of

http://doc.rero.ch

the polymer wall as shown in Figure S2. The large band in the range of 1000-1500 cm^{-1} can be assigned to vibration of Si-containing bonds. The peak around 2400 cm^{-1} visible in all spectra is attributed to CO_2 from the environment but could also partially due to the presence of some residual carbonized polymer.

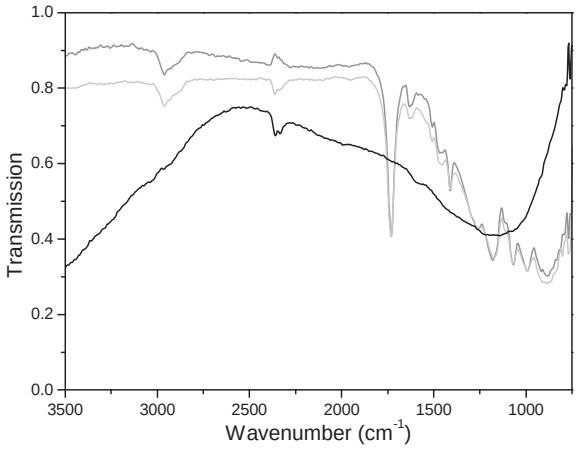

Figure SI-5. MIR spectra in transmission of HU structure in polymer only (dark gray line), after TiO_2 ALD (light gray line) and Si CVD (black line).

http://doc.rero.ch